

© Copyright 1996 American Meteorological Society (AMS). Permission to use figures, tables, and brief excerpts from this work in scientific and educational works is hereby granted provided that the source is acknowledged. Any use of material in this work that is determined to be “fair use” under Section 107 of the U.S. Copyright Act or that satisfies the conditions specified in Section 108 of the U.S. Copyright Act (17 USC §108, as revised by P.L. 94-553) does not require the AMS’s permission. Republication, systematic reproduction, posting in electronic form on servers, or other uses of this material, except as exempted by the above statement, requires written permission or a license from the AMS. Additional details are provided in the AMS CopyrightPolicy, available on the AMS Web site located at (<http://www.ametsoc.org/AMS>) or from the AMS at 617-227-2425 or copyright@ametsoc.org.

Permission to place a copy of this work on this server has been provided by the AMS. The AMS does not guarantee that the copy provided here is an accurate copy of the published work.

COMPARISON OF THE PERFORMANCE OF THE INTEGRATED TERMINAL WEATHER SYSTEM (ITWS) AND TERMINAL DOPPLER WEATHER RADAR (TDWR) MICROBURST DETECTION ALGORITHMS*†

Timothy J. Dasey, Margita L. Pawlak, Mark A. Isaminger, Michael F. Donovan

Lincoln Laboratory
Massachusetts Institute of Technology

1. INTRODUCTION

Microbursts are intense downdrafts produced within thunderstorms. When these downdrafts impact the ground, the resulting windshear can pose grave dangers to aircraft at low altitudes (Fujita and Byers, 1997, National Research Council, 1983). Microbursts are often associated with heavy rainfall, but can occur without surface rainfall (Wolfson, 1988).

The Terminal Doppler Weather Radar (TDWR) is intended to provide wind shear awareness for pilots and air traffic controllers by detecting microbursts and other wind shear disturbances in the terminal area (Turnbull et. al., 1989). The TDWR is a pencil beam radar which estimates surface reflectivity, doppler velocity, signal-to-noise, and spectrum width data approximately every minute at the surface for a scan sector that includes the runways and approach and departure corridors. Aloft scans are conducted in the intervening time, requiring about 2.5 minutes to collect a complete volume sample over the sector region. The TDWR microburst detection algorithm will locate microbursts within about 20 nautical miles of the radar.

The TDWR microburst algorithm provides graphical alerts as icons on a map of the terminal area, and as text alerts for each runway. TDWR performance has always been evaluated by comparing the output icons with a "truth" data set created by expert meteorologists. In general, the TDWR algorithm identifies microbursts with > 90% Probability of Detection (POD) and < 10% Probability of False Alarm (PFA), when output algorithm icons are scored (Merrit et. al., 1989).

Corresponding Author Address: Timothy J. Dasey, M.I.T. Lincoln Laboratory, 244 Wood St., Building S, Lexington, MA 02173-9185; email timd@ll.mit.edu

* This work is sponsored by the Federal Aviation Administration's Aviation Weather Development Program. The views expressed are those of the author(s) and do not necessarily represent the official policy or position of the U.S. Government.

† Opinions, interpretations, conclusions, and recommendations are those of the authors and are not necessarily endorsed by the United States Air Force.

The Integrated Terminal Weather System (ITWS) development presented the opportunity to enhance the windshear characterization capabilities of the TDWR and capitalize on the knowledge gained since the TDWR was developed. Much of our increased understanding of microburst impact on aircraft is due to the analysis of data from instrumented aircraft penetrations of microbursts, coincident with TDWR testbed operation (Matthews et. al., 1994). The microburst penetration flights were conducted by NASA Langley, the University of North Dakota (UND), and several manufacturers of forward-looking wind shear detection systems.

These microburst penetrations helped scientists to conclude that an aircraft energy loss rate measure, deemed the F-factor (Bowles, 1990), is a good indicator of the microburst aviation hazard. When the basic F-factor equation is modified for estimation with a Doppler radar, the total F-factor (F_T) can be expressed as

$$F_T = K' \frac{\Delta V}{\Delta R} \left(\frac{GS}{g} + \frac{2h}{TAS} \right) \quad (1)$$

where K' is a constant, ΔV is the headwind/tailwind velocity difference, ΔR is the distance over which the velocity difference is computed, GS is the groundspeed of the aircraft, TAS is the true air speed of the aircraft, g is the gravitational constant, and h is the height of the radar beam.

The important characteristic of equation (1) is that the F-factor is proportional to the shear across the event ($\Delta V / \Delta R$), rather than the loss (ΔV). The TDWR microburst algorithm internally uses loss as a primary indicator of the microburst hazard. Clearly both loss and shear are important. A very strong shear may not be very hazardous if it is localized to a very small area. A very large loss value may not indicate a very hazardous event if the loss is spread over a large area, so that the shear through the event is small. The ITWS Microburst Detection algorithm combines both hazard criteria by requiring an event to have a minimum level of shear for it to be considered hazardous, while also requiring the high shear to have sufficiently large area.

The ITWS Microburst Prediction algorithm was developed to forecast the onset or intensification of microbursts. The Microburst Prediction algorithm relies on the ITWS Microburst Detection algorithm to provide continuous feedback on its prediction accuracy. This feedback requires detections which are more spatially confined than those from the TDWR algorithm. The ITWS Microburst Detection algorithm can satisfy this Microburst Prediction requirement by warning about intense shear regions, which typically are small in area.

This paper describes the designs of the TDWR and ITWS Microburst Detection algorithms, and compares their performances in the Orlando, FL and Memphis, TN environments. This is the first study in which the performance of the TDWR and ITWS microburst detection algorithms are compared using an identical data set and a common set of truth criteria. Examples are presented illustrating common scenarios which create the performance differences. Detail is presented on the impact of the ITWS VIL (Vertically Integrated Liquid water) test in reducing algorithm false alarms. This algorithm feature is currently being considered as a retrofit to the TDWR algorithm.

2. ALGORITHM DESCRIPTIONS

The TDWR radar provides the base data upon which both the TDWR and ITWS microburst algorithm alerts are based. The TDWR is a C-band pencil beam radar which provides surface reflectivity, doppler velocity, signal-to-noise, and spectrum width data approximately every minute at the surface for a scan sector that includes the runways and approach and departure corridors. Aloft scans are conducted in the intervening time, requiring about 2.5 minutes to collect a complete volume sample over the sector region. Base data estimates are provided every 1 degree in azimuth and 150 m in range. Several data quality algorithms (including clutter suppression, point-target editing, ground clutter residue removal, range obscuration editing, and velocity unfolding) are applied to the radar base data prior to their use by the TDWR or ITWS product generation algorithms. Microburst alerts from each algorithm are provided in iconic form out to about 20 nm from the radar, and in text form for each active arrival and departure runway corridor.

2.1. TDWR Microburst Detection Algorithm

The primary algorithm for detecting microburst signatures in the TDWR software is the *build divergence regions* algorithm. This algorithm uses as input the velocity data from the one minute update rate sur-

face scans. For each surface scan, the algorithm finds shear segments by locating series of increasing values. Each of these shear segments is checked for adequate length and slope of shear. Segments which pass these tests are associated with shear segments from neighboring radials to form two-dimensional regions of divergence. These divergence regions are checked for adequate area, number of segments, and maximum segment strength. Remaining divergence regions are sent to the *identify surface outflows* algorithm which checks the divergence regions for strength and temporal correlation with divergence regions from previous surface scans to determine which regions will become surface outflows and which will become candidate outflows. These outflow regions are sent to the *identify surface microbursts* algorithm which declares all of the surface outflows and the candidate outflows that are associated with a microburst feature aloft to be microburst outflows. These microburst outflows are described by a bounding box which is made up of two pairs of points (in km east and north of the radar) which indicate the corners of a rectangle enclosing the microburst outflow region. Microburst shapes are created from these microburst outflows and are sent to the DFU (display function unit). See Figure 1 for a diagram of surface outflow detection processes.

To reduce the number of false alarms, the microburst outflows that are created by the *identify surface microbursts* algorithm can be checked for correlation with a storm cell or a low reflectivity cell before being issued. Storm Cells are created by vertically correlating reflectivity regions created using a 30 dBZ threshold level. These reflectivity regions, which are generated for each of the aloft scans, have met criteria for reflectivity, size, and altitude, and are vertically correlated using a normalized centroid separation test. The normalized centroid separation test calculates the distance between the centroids of each reflectivity region and divides this distance by the sum of their mean radii. Once all possible reflectivity regions have been vertically correlated or discarded, each storm cell is checked to verify that its vertical extent is greater than or equal to a threshold value. A pair of points (in km east and north of the radar) that indicate the corners of a rectangle which enclose the storm cell region are described as a bounding box. If the centroids of the microburst outflow and the Storm Cell are sufficiently close, or the bounding boxes overlap enough, the microburst outflow is considered valid and retained. Low Reflectivity Cells are created at lower reflectivity levels (e.g., 15 dBZ instead of 30 dBZ) and can be used

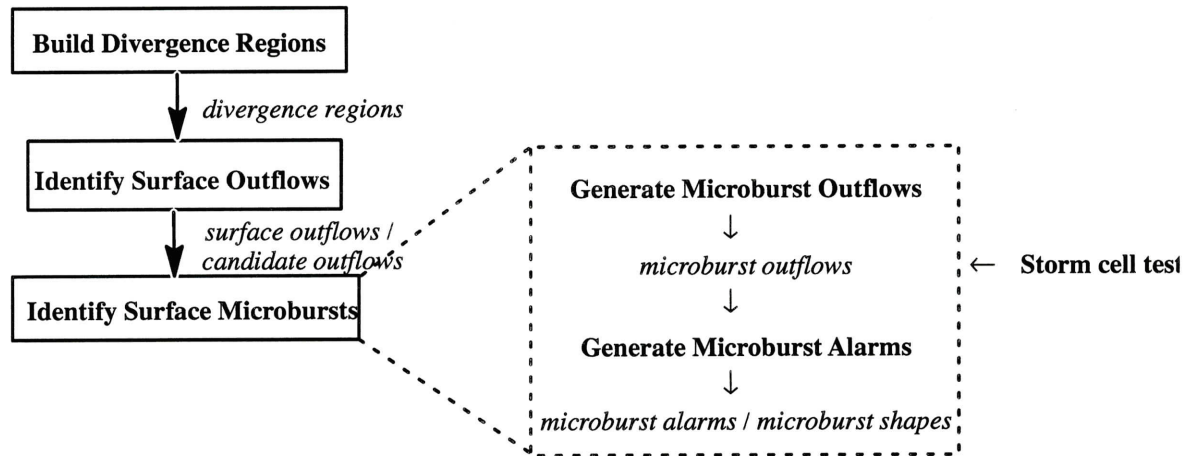


Figure 1. Algorithmic flow for surface microburst detection. Algorithms are in boxes and intermediate outputs are in italics. The Identify Surface Microbursts algorithm is shown in greater detail in the box on the right.

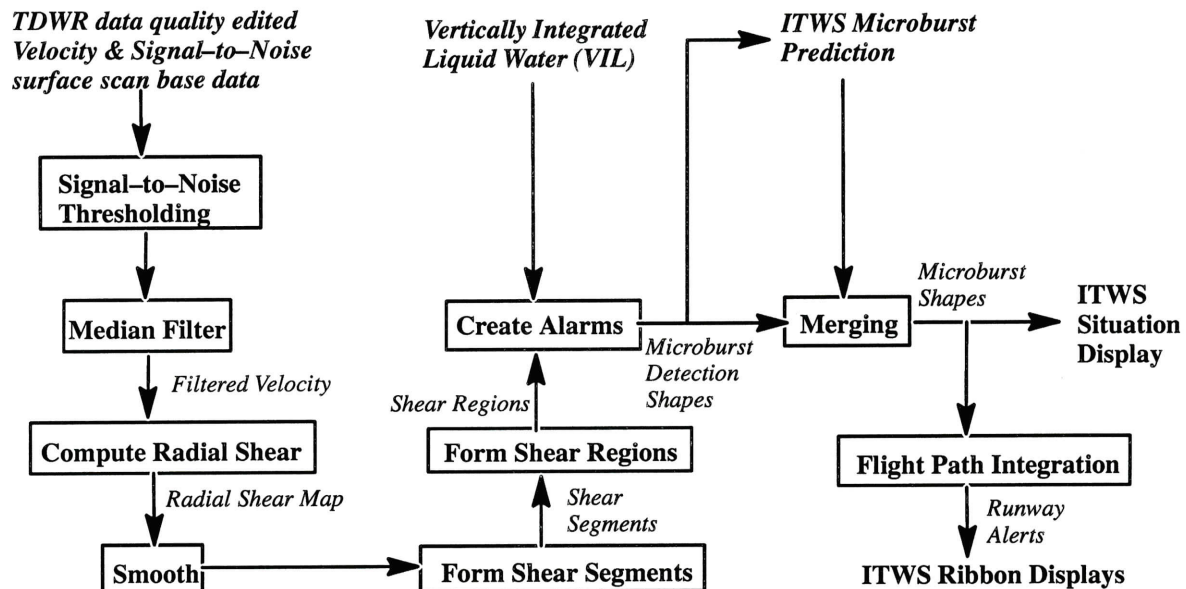


Figure 2. Processing components of the ITWS Microburst Detection Algorithm

instead of Storm Cells to validate microburst outflows in low reflectivity environments.

Alerts are presented graphically to the users as icons on a map of the terminal area, or as text alerts for each runway. Alerts ≥ 15 kts. and < 30 kts. are termed windshear alerts, and are represented by unfilled red shapes on the graphic display. Alerts ≥ 30 kts. are termed microburst alerts and are represented by solid red-filled shapes on the graphic display.

The text alerts are computed by summing the average shear across an icon over the length of overlap with a runway buffer region. This process is known as shear integration. The ribbon alert then has a value

proportional to the degree to which the event is centered on the flight path.

2.2. ITWS Microburst Detection Algorithm

The ITWS Microburst Detection Algorithm is comprised of several subcomponents, depicted in Figure 2. A signal-to-noise threshold is applied to velocity base data, and then optionally median filtered prior to the estimation of the radial shear. The radial shear value of each gate is computed as the slope of a linear regression fit to the Doppler velocities in an ~ 1 km window centered on the analysis gate. The 1 km window length is chosen to conform with the parameters used in the airborne forward-looking systems. Shear values are considered invalid if the velocity values

used in the regression fit are insufficiently correlated or too few valid velocity values are available within the analysis window. Adjacent radials may be used in the shear computation through selection of a site adjustable parameter. The use of adjacent radials acts to smooth noisy radar velocity data.

Segments are created by grouping contiguous gates along a radial which exceed a certain threshold level of divergent (positive) shear. Each segment is then extended until either (a) the average shear along its length falls below the threshold, (b) a gate with a negative shear value is encountered, (c) an excessive percentage of the segment gates have subthreshold values, or (d) an excessive number of consecutive invalid shear values are found. In this way, a segment is not constructed unless a minimum shear is present, but the length of the segment is not rigidly tied to the points above threshold. All segments must exceed a minimum length threshold. Figure 3 gives an example of the segment building process for a shear threshold value of 5 m/s/km.

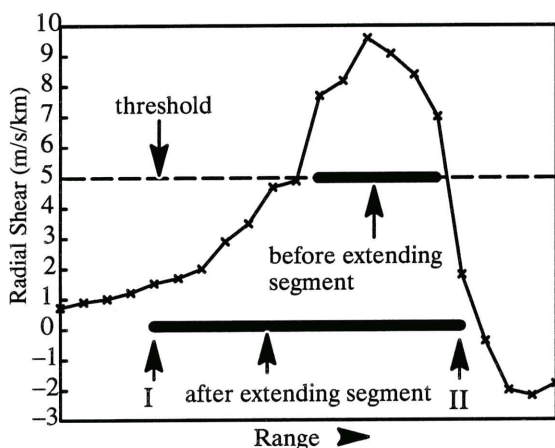


Figure 3. ITWS segment forming process. The final segment endpoint I was placed by condition (a), and endpoint II was placed by condition (b) in the text.

Two-dimensional representations of high shear regions are formed by grouping together shear segments on adjacent radials which overlap in range by a specified amount. Regions are fit to iconic representations using an optimization routine which minimizes the distance between the segment ends and the icon perimeter. The icon is usually chosen to be a circle, unless the aspect ratio (azimuthal width / radial length) of the region exceeds a threshold. If it does, a more elliptical "racetrack" shape is fit to the region. The shear region is discarded for insufficient area or number of segments.

Site-adaptable parameters can be chosen to run the segment and region forming processes at several

different shear threshold levels. The regions at different threshold levels are then spatially associated with one another and the association tree from the lowest threshold level is searched for multiple shear regions at higher threshold levels. The regions are split so that multiple shear peaks are not present within a region.

After regions have been created, confirming evidence for a microburst is sought by requiring a minimum level of Vertically Integrated Liquid water (VIL) within a minimum distance from the center of the icon. The minimum VIL threshold can be chosen very low for environments with prevalent "dry" microbursts.

VIL is the integration of the liquid water equivalent reflectivity in a vertical column. VIL is calculated for every "volume" of reflectivity, where a volume is defined to be a collection of the surface and aloft tilts ending with the tilt with the highest elevation angle. Each "volume" contains data from the last 2-3 minutes. VIL is calculated for a 1 km by 1 km grid covering the entire hazardous scanning sector from a minimum range to a range equal to the maximum range that microbursts are detected. The minimum range constraint is a function of the elevation angle of the highest scan.

Reflectivity from every polar scan of the "volume" is converted to liquid water and mapped to a 3-D Cartesian grid. The conversion from reflectivity to liquid water assumes a Marshall-Palmer (Marshall and Palmer, 1948) drop-size distribution so that the relationship between liquid water and reflectivity is:

$$\text{liquid water} = 3.44 \times 10^{-3} [Z]^{4/7}$$

Interpolation of missing data is performed using a Cressman weighting scheme which uses liquid water values from a defined region surrounding the missing point. The liquid water values in each "column" are integrated forming a 2-D grid of VIL.

At the time that the ITWS algorithm was being developed and operationally tested, the TDWR radars were just beginning to be commissioned nationwide. Controllers were concerned about any potential retraining at that time in the interpretation of windshear alerts. For this reason, the ITWS alerts are put out in the same format as the TDWR alerts. Loss values for each shape is the maximum loss of all segments belonging to that shape. The segment loss values are found by imagining another segment extension in a manner analogous to the procedure discussed above (although with a weaker shear threshold level of 2.5 m/s/km) and computing the endpoint velocity difference of this imaginary segment.

Those regions which pass the VIL test, and have losses which exceed 15 kts., are merged with any concurrent microburst predictions and sent to the ITWS Situation Display (SD). They are also sent to the shear integration algorithm which operates identically to the TDWR version to compute runway specific text alerts.

3. PERFORMANCE ANALYSIS

TDWR and ITWS algorithm alerts can be scored either by analyzing the icons presented on the graphical display, or by assessing the runway specific alerts on the controller ribbon displays. The ribbon display alerts are the only alerts actually forwarded to the pilots, and as such are more operationally relevant than the iconic alerts. Runway alert scoring also eliminates the ambiguities in algorithm icon scoring due to threshold selection in the extent of overlap between algorithm alerts and truth regions. Traditionally, the TDWR algorithm has been evaluated using the iconic alerts. This study examines the performance of both algorithms using runway alerts.

3.1. Data Sets

Base data and microburst product archives were collected daily and archived for off-line analysis from both the Memphis, TN and Orlando, FL ITWS prototypes. Days on which the strongest microburst runway impact occurred, and for which both TDWR and ITWS product archives were available, were chosen from the ITWS Demonstration and Validation (Dem-Val) periods in Orlando and Memphis in 1994. The times and dates used for each site are shown in Tables 1 and 2. Care was taken to include periods of inactive microburst activity for each day to properly assess algorithm false alarm rates. The Lincoln Laboratory testbed algorithm software was used to generate ITWS alerts. The TDWR alerts were generated by running real-time TDWR version 5A alerts through an offline Lincoln version of the shear integration flight path alerting software. The shear integration algorithm is part of TDWR version 5B software.

Orlando Case Date	Time Period (GMT)
14 July 1994	19:36 – 21:39
16 July 1994	20:10 – 21:30
21 July 1994	16:40 – 17:46
27 July 1994	20:05 – 20:38
28 July 1994	18:42 – 19:19
30 July 1994	20:55 – 21:38
5 August 1994	20:05 – 21:49

6 August 1994	18:07 – 19:12
17 August 1994	18:52 – 19:29, 23:07 – 23:49

Table 1. Listing of the Orlando time periods selected for analysis.

Memphis Case Date	Time Period (GMT)
9 June 1994	17:50 – 18:26
16 June 1994	21:16 – 21:48
26 June 1994	12:03 – 12:55
30 June 1994	15:47 – 16:11
4 July 1994	18:42 – 19:44

Table 2. Listing of the Memphis time periods selected for analysis.

3.2. Truth Generation

Benchmark truth data for algorithm scoring were generated for each time period listed in Tables 1 and 2 by an expert meteorologist with experience in the interpretation of Doppler weather radar data. The truther examined each runway corridor and identified the intensity and location of any wind shear observed for the current flight path configuration. The analyses were performed using Doppler velocity, radial shear, and Vertically Integrated Liquid water (VIL) images.

An event was classified by the truther as a wind shear or microburst event if the following criteria were met.

- Events must contain a continuous region of at least 4.0 m/s/km of radial shear for several radials in azimuth and for at least 0.5 km along the flight path.
- The maximum velocity difference (loss) along a radial must be at least 7.8 m/s (15 kts.) over a distance of 3 km or less.
- A VIL value of at least 5 kg/m² must be within 2 km of the event area boundary.

Once the above criteria were met, the strength of the event was recorded as the maximum loss within a fixed distance of the runway flight path. This distance was chosen to conform to the runway buffer regions used in the shear integration routines. Most of the truthed data was for flight paths nearly along a radar radial. For those runways which were not oriented along a radial, an assumption of circular symmetry of the microburst was used, so that truth data could be constructed using the available TDWR radar data.

3.3. Scoring and Performance Metrics

The truth data were compared with the microburst alerts and compiled into contingency tables using the

methods and tolerances described by Cole and Todd (Cole and Todd, 1993). A five knot tolerance was used to build the contingency tables to allow for inaccuracies in the truth data. In the contingency table approach, the alerts are categorized as they are in operational use: as a null alert (NULLA), windshear alert (WSA), or microburst alert (MBA). The truths are categorized as a null truth (NULLT), windshear truth (WST), or microburst truth (MBT). The classification categories using the 5 kt truth tolerance are shown in Figure 4.

	TRUTH VALUE (knots)			
	0	10	20	25 35
0	NULLA/ NULLT		NULLA/ WST	
15	WSA/ NULLT	WSA/WST		WSA/MBT
30	MBA/ NULLT	MBA/WST	MBA/MBT	

Figure 4. Alert and truth classifications for entry into the contingency table.

The performance assessment of the ITWS and TDWR microburst detection algorithms were completed using the metrics of Probability of Detection (POD) and Probability of False Alarm (PFA). POD is defined as the fraction of truth events for which an algorithm alert was generated. PFA is defined as the fraction of algorithm alerts not supported by truth. These performance statistics were generated for both the wind shear alert (WSA) and microburst alert (MBA) levels. Additional measures of performance include the Probability of Overwarning (POW) and the Probability of Underwarning (PUW). POW indicates the fraction of alerts incorrectly declared microburst alerts when the truth indicated a wind shear alert was appropriate. PUW indicates the fraction of alerts incorrectly declared wind shear alerts when the truth indicated a microburst alert was appropriate. The performance statistics are defined as follows:

POD (loss | WS): the probability that either a WSA or MBA was issued given a WST.

POD (loss | MB): the probability that either a WSA or MBA was issued given a MBT.

POD (MB | MB): the probability that a MBA was issued given a MBT.

POD (loss | loss): the probability that a WSA or MBA was issued given a WST or a MBT.

PFA (false WS | WS): the probability that a WSA was issued given a NULLT.

PFA (false MB | MB): the probability that a MBA was issued given a NULLT.

PFA (false loss | loss): the probability that a WSA or a MBA was issued given a NULLT.

PUW: the probability that an alert was issued at a lower alert level than necessary.

POW: the probability that an alert was issued at a higher alert level than necessary.

3.4. Operational Requirements

The requirements for the ITWS microburst detection algorithm, as stated in the ITWS Operational Requirements Document (ORD) are as follows.

- The ITWS microburst product should be capable of a probability of detection for wind shear alerts of 0.90, and for microburst alerts of 0.95 on a runway corridor basis.
- The probability that a windshear or microburst alert will be false should be less than 0.05.
- Windshear loss estimates should be within ± 5 knots or 0.20 percent of the actual loss, whichever is greater, 70% of the time.

3.5. Performance of ITWS and TDWR Algorithms

Algorithm alert and truth pairs were classified using the boundaries shown in Figure 4 for all of the data in Tables 1 and 2. Contingency tables, showing the frequency count for these classifications, were maintained for each algorithm. The values from these contingency tables were used to generate the statistics described in section 3.3, which are shown in Table 3. The Memphis data set contains very few events of microburst intensity, so ITWS data was also scored using an expanded data with additional data from 1993 and 1995. The ITWS performance results from this exercise are shown in parentheses in Table 3. TDWR algorithm output data was not readily available for this expanded data set. In general, very little difference can be noted in the ITWS performance with the additional Memphis data.

As can be seen from Table 3, ITWS meets all of its operational requirements both in Memphis and Orlando, with a 99%+ POD for microburst alert level events, and a 95%+ POD for windshear alert level

events. The ITWS PFA's for all alert levels are 3% or below, and over 75% of alerts are within 5 kts. or 20% of the actual loss. The TDWR algorithm POD performance numbers are generally comparable, but the TDWR shows a much larger PFA and a larger probability of overwarning. The increased false alarm rates shown for the TDWR are largely the result of three factors:

- The VIL test used by the ITWS algorithm is a more accurate indicator of microburst forcing.
- The TDWR algorithm often generates larger microburst shapes than the ITWS algorithm, which can intrude into the flight path corridor and generate additional alerts.
- The TDWR algorithm does not directly incorporate the shear criterion of the truth set in generating alerts.
- TDWR Build 5A does not include changes which probably would reduce the TDWR false alarm rates (Klinge-Wilson et. al., 1996). Specifically, changes were made to the minimum number of segments for a divergence region, the minimum number of segments for an alarm, the minimum alarm velocity, and the storm centroid distance in Build 5B. In addition, a parameter was included to test for overlap between the storm cell bounding box and microburst outflow bounding box. The new parameters were stricter than those used in Build 5A.

The ITWS algorithm was written with the benefit of the development of the airborne forward looking windshear detection systems, during which extensive work was performed showing that the hazard to the aircraft is best characterized by analysis of shear instead of loss. As the TDWR algorithm was developed prior to this work, it is based primarily on detecting loss regions. The resulting shapes are typically larger and more numerous than the regions of hazardous shear. The next section discusses the differences between the alerts from the ITWS and TDWR algorithms.

4. PERFORMANCE DIFFERENCES

4.1. Impact of VIL Test

Many of the TDWR false alarms can be attributed to the lack of specificity of the storm cell test used by that algorithm. Figure 5 shows a typical situation where the more lenient storm cell test would allow a microburst alert, while the VIL test would prevent the algorithm from issuing the alert.

The benefit of the VIL test has been objectively studied for consideration of adding it to the TDWR microburst detection software. The relative perfor-

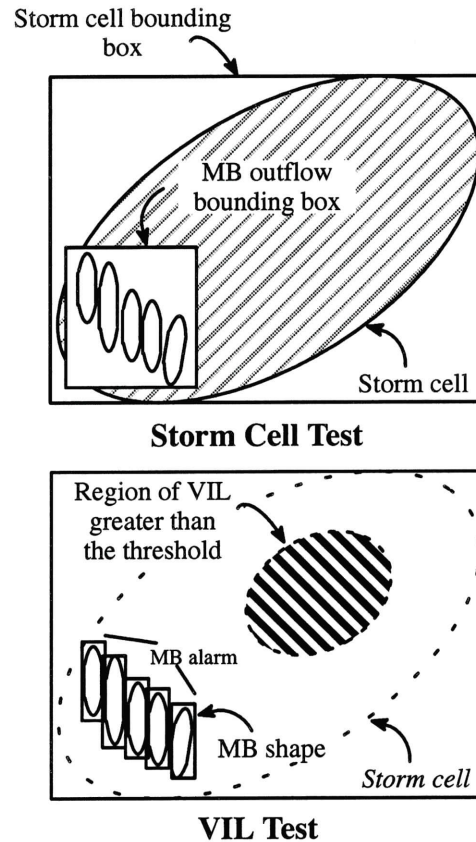


Figure 5. An explanation for how the VIL test provides better specificity than the storm cell test. The storm cell and microburst outflow centroids are close enough and the bounding boxes overlap enough that the storm cell test allows the shapes to be output. However, in the lower frame, the region of VIL above the threshold value is not sufficiently close to the microburst shapes and the shapes are not output.

mances of the 5B/V35 microburst detection algorithm software (with and without the VIL test) were compared to assess the effect of the proposed enhancement. For this evaluation, we analyzed base data and wind shear/microburst detections from TDWRs located in Oklahoma City (OEX), Dallas Love (DAL), Memphis (MEM), Washington National (DCA) and Denver (DEN). The validity of each windshear and microburst detection was determined by an expert radar meteorologist who examined the alarm location with respect to the TDWR reflectivity and velocity field. Alarms that were not associated with a reflectivity structure were classified as false, unless they were caused by either gravity waves or divergence behind a gust front (DBGF). Alarms associated with these two features were treated as neutral and the detection algorithm was not penalized.

The impact of using the VIL test in the TDWR microburst detection algorithm is shown in Table 4. The

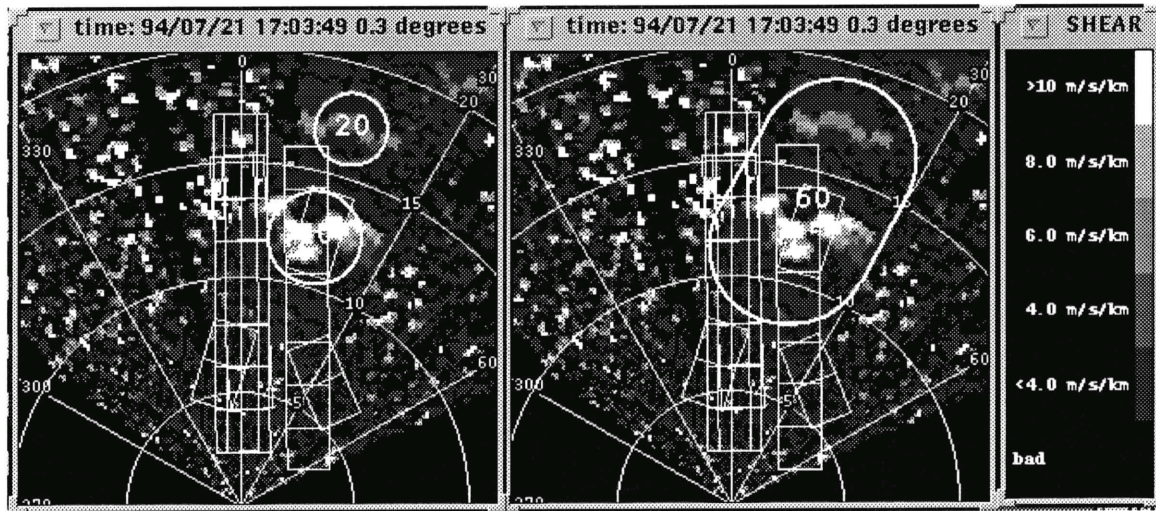


Figure 6. Example of the smaller shapes usually issued by the ITWS algorithm (left) versus the TDWR algorithm (right) for an Orlando event. The background colors represent ITWS-computed radial shear, and the airport arenas are shown as box overlays. The intensities are shown in knots at the center of each alert.

false alarms were divided into two strength categories; e.g., wind shear (WS) for those events less than 30 knots and microburst (MB) for those events 30 knots or greater. For this data set, the 5B/V35 algorithm produced 277 false alarms. An analysis of the false events showed many were located in regions of weak divergence either outside or on the edge of a reflectivity cell. These areas were contaminated with one or several pixels of noise which produced a signature that satisfied the velocity threshold requirement. The algorithm is sensitive to noise contamination and therefore does not adequately eliminate events of this type without an aggressive reflectivity validation test. In terms of the intensity, the majority of the false alarms were classified as wind shears (243/277 or 88 percent). The two days with the highest false alarm rates were from OEX (5-08-93 and 5-15-93) and the VIL test was particularly successful at eliminating false alarms on these days. This improvement was significant since the false alarm rate at this site was significantly higher than the specification, e.g., 18 percent (Vasiloff, 1993). Overall, the VIL test removed approximately one-third (94/277) of the false alarms in this data set (see Table 4). According to Klinge-Wilson et. al. (Klinge-Wilson et. al., 1996), the 5B/V35 false alarm rate at DCA was marginal (9.5 percent), so the new test would decrease the false alarm rate at this site even further. Finally, we expect the false alarm rate at sites like DAL to be high due to moving clutter breakthrough, increasing the need for the more stringent reflectivity checking criteria of the VIL test.

In terms of detection performance, there were no wind shear or microburst events removed by the VIL

test at the wet microburst sites. This factor is significant since the parameter changes installed with 5B/V35 resulted in approximately a 2 percent reduction in detection performance at MEM, DCA and MCO (Klinge-Wilson et. al., 1996). However, the VIL test did have a negative impact on detection performance at dry microburst sites. Based upon the one case from DEN that was examined, the VIL test removed the only valid wind shear event, which persisted for four minutes. It is expected that this trend would prevail in low reflectivity events since there is very little vertical structure in the reflectivity column and hence little or no VIL. The wind shear detection capability at dry sites like DEN is already marginal (Merritt, 1989) and this test would reduce it even further. Based upon these results, it was determined that the VIL test was not appropriate in this type of environment. Use of the VIL test can be disabled at sites where dry microbursts may occur by setting the VIL threshold to zero.

4.2. Areal Extent of Alerts

The more stringent shear criterion of the ITWS algorithm usually results in smaller iconic alerts from ITWS than from TDWR. An example is shown in Figure 6. Many of the TDWR false alarms in Table 3 are the result of excessively large TDWR shapes, which are more likely to overlap a runway corridor. Notice that much of the warning area of the TDWR alert is in areas of weak shear. The larger TDWR shape results in runway alerts to all three MCO runways (and overwarns on runway 17), while the ITWS alert properly alerts only runway 17 with a 40 kt loss on approach. In reality, the TDWR alert merged two distinct micro-

burst events (as seen from the background shear), resulting in a single 60 kt shape, versus the distinct 20 kt and 40 kt shapes from ITWS.

4.3. Handling of Weak Shear Alerts

The ITWS algorithm shear threshold of 4.0 m/s/km is more stringent than tests applied by the TDWR algorithm. In many cases, a weak windshear event (15–20 kts.) which was alerted by the TDWR algorithm was not alerted by the ITWS algorithm. These events were spread over a large enough area that the shear at any point in the event is (by F-factor analysis) presumably not dangerous to aircraft. These events were deemed TDWR false alerts in this scoring procedure.

5. DISCUSSION

The TDWR is instrumental in improving airport safety through timely warnings of hazardous wind shear. Experience has shown that windshear alerting algorithms must maintain a high probability of detection, while at the same time keep the false alarm rate low so that the users are confident in the alerts. The ITWS microburst detection algorithm was developed to promote the successful implementation of a microburst prediction product, and to capitalize on the knowledge gained about the microburst hazard to aviation since the TDWR algorithms were developed.

This study illustrates the improvements of the ITWS algorithm over the TDWR algorithm in reducing the number of algorithm false alerts. It is important to note that the ITWS algorithm outperforms the TDWR algorithm in this respect in part because the criteria for hazardous windshear has been changed from the time the TDWR algorithm was developed. The shear-based approach of the ITWS algorithm applies more stringent criteria for alerting, particularly for weak events. ITWS alerts tend to be less numerous and smaller.

Some of the increase in false alarm rate and overwarning shown by the TDWR algorithm may be attributable to differences between versions 5A and 5B of the algorithm. It is also clear that much of the increase in runway alert false alarms from the TDWR algorithm were not corrected by Build 5B. Extensive analysis of the effect of the VIL test on TDWR algorithm performance indicates that this test is likely a large factor in the improved ITWS algorithm performance. The more stringent shear criterion of the ITWS algorithm results in more highly localized alerts than from the TDWR algorithm, which will tend to reduce runway alert false alarms.

Additional work remains to optimize the performance of the ITWS Microburst Detection algorithm. Narrow bands of azimuthally aligned shear often result in excessively large shapes. It is expected that the use of the region splitting portion of the algorithm (which is currently not selected for use at ITWS prototype facilities) can remove this problem. Weak windshear alerts are also observed on the edges of storms, particularly in the presence of noisy velocity data, such as is found at DAL.

There are still issues regarding the generation of ground-based microburst alerts which require some attention by an appropriate user group. Among these issues are the ground-based alert format and the windshear threshold levels. A potential conflict exists between airborne systems, which rely on F-factor for alert generation, and ground-based systems, which still specify alerts as windspeed loss. The 15 kt minimum alert threshold of the ITWS algorithm may also be too weak, unless other algorithms, such as ITWS Microburst Prediction, have evidence that the event is gaining intensity.

REFERENCE

- Bowles, R. L., 1990: "Reducing Windshear Risk Through Airborne Systems Technology", 17th Congress on the Aeronautical Sciences, Stockholm, Sweden, Sep. 9–14.
- Cole, R., and R. Todd, 1993: "A Comparative Performance Study of TDWR/LLWAS 3 Integration Algorithms for Wind Shear Detection", Proc. 5th International Conference on Aviation Weather Systems, Vienna, VA (American Meteorological Society, Boston, MA), pp. 103–107.
- Fujita, T. T. and H. R. Byers, 1977: "Spearhead Echo and Downburst in the Crash of an Airliner", *Mon. Weather Rev.* 105: 129.
- Klinge-Wilson, D., M. Isaminger, and C. Keohan, 1996: "Report on Product Performance for the Terminal Doppler Weather Radars at Washington National Airport, and Memphis and Orlando International Airports," MIT Lincoln Laboratory Project Report ATC-246 (available through the National Technical Information Service, Springfield, VA 22161), publication pending.
- Marshall, J.S. and W.M. Palmer, 1948: "The distribution of raindrops with size," *J. Meteor.*, 5, 165–166.
- Matthews, M. P., S. D. Campbell, and T. J. Dasey, 1994: "Cockpit Weather Information (CWI) Program Summary Report for FY1993", M.I.T. Lincoln Laboratory Project Report NASA/L-1 (available through the National Technical Information Service, Springfield, VA 22161).
- Merritt, M.W., D. Klinge-Wilson and S.D. Campbell, 1989: "Wind Shear Detection with Pencil-Beam Radars," *Lincoln Laboratory Journal* 2, MIT Lincoln Laboratory, 483.

National Research Council, 1983: "Low–Altitude Wind Shear and its Hazard to Aviation", National Academy Press, Washington, D.C.

Turnbull, D., J. McCarthy, J. Evans, and D. Zrnic, 1989: "The FAA Terminal Doppler Weather Radar (TDWR) Program", Proc. 3rd Intl. Conference on Aviation Weather Systems, Anaheim, 30 Jan – 3 Feb (Amer. Meteor. Soc.), p. 414.

Vasiloff, S., 1993: "Terminal Doppler Weather Radar (TDWR) Operational Test and Evaluation: Final Report on Weather–Detection Performance", National Severe Storms Laboratory, Techniques Development Branch, Storm–Scale Research and Applications Division, Norman, Oklahoma.

Wolfson, M., 1988: "Characteristics of Microbursts in the Continental United States", *Lincoln Laboratory Journal* 1(1): 49–74.

Statistic	Orlando		Memphis	
	ITWS	TDWR	ITWS	TDWR
POD(loss WS)	0.98	0.95	0.95 (0.95)	0.89
POD(loss MB)	1.00	1.00	1.00 (0.99)	1.00
POD(MB MB)	0.95	0.98	0.92 (0.92)	1.00
POD(loss loss)	0.99	0.96	0.95 (0.96)	0.90
PFA(false WS WS)	0.03	0.26	0.01 (0.02)	0.17
PFA(false MB MB)	0.00	0.05	0.00 (0.00)	0.08
PFA(false loss loss)	0.03	0.19	0.01 (0.01)	0.16
POW	0.15	0.35	0.08 (0.07)	0.24
PUW	0.01	0.01	0.01 (0.02)	0.00
P(alert w/in ± 5 kts. or 20% of loss)	0.78	0.56	0.89 (0.76)	0.71

Table 3. Runway alert performance statistics for the ITWS and TDWR algorithms.

		STORM CELL TEST			VIL TEST		
Date	Site	# WS FA	# MB FA	Total FA	# WS FA	# MB FA	Total FA
4–28–93	OEX	0	0	0	0	0	0
5–08–93	OEX	47	11	58	21	7	28
5–09–93	OEX	3	0	3	3	0	3
5–15–93	OEX	35	12	47	14	9	23
6–26–94	MEM	33	2	35	23	2	25
9–26–94	DCA	27	0	27	20	0	20
9–27–94	DCA	38	1	39	37	1	38
11–01–94	DCA	13	0	13	13	0	13
11–21–94	DCA	15	2	17	5	0	5
08–29–95	DAL	32	6	38	23	5	28
	Totals	243	34	277	159	24	183

Table 4. Comparison of the false alarms generated by the TDWR algorithm using the storm cell test and the VIL test.